Multiple Oscillatory Push–Pull Antagonisms Constrain Seizure Propagation

Haiteng Jiang, PhD,[1] Zhengxiang Cai, MS,[1] Gregory A. Worrell, MD, PhD [ORCID],[2] and Bin He, PhD [ORCID][1]

Objective: Drug-resistant focal epilepsy is widely recognized as a network disease in which epileptic seizure propagation is likely coordinated by different neuronal oscillations such as low-frequency activity (LFA), high-frequency activity (HFA), or low-to-high cross-frequency coupling. However, the mechanism by which different oscillatory networks constrain the propagation of focal seizures remains unclear.

Methods: We studied focal epilepsy patients with invasive electrocorticography (ECoG) recordings and compared multilayer directional network interactions between focal seizures either with or without secondary generalization. Within-frequency and cross-frequency directional connectivity were estimated by an adaptive directed transfer function and cross-frequency directionality, respectively.

Results: In the within-frequency epileptic network, we found that the seizure onset zone (SOZ) always sent stronger information flow to the surrounding regions, and secondary generalization was accompanied by weaker information flow in the LFA from the surrounding regions to SOZ. In the cross-frequency epileptic network, secondary generalization was associated with either decreased information flow from surrounding regions' HFA to SOZ's LFA or increased information flow from SOZ's LFA to surrounding regions' HFA.

Interpretation: Our results suggest that the secondary generalization of focal seizures is regulated by numerous within- and cross-frequency push–pull dynamics, potentially reflecting impaired excitation–inhibition interactions of the epileptic network.

ANN NEUROL 2019;86:683–694

Epilepsy is one of the most prominent neurological diseases,[1] and it is well established that focal epilepsy is a network disease.[2] Although epilepsy is often treated with medication, in patients with drug-resistant epilepsy, the epileptogenic zone (the minimum volume of tissue that needs to be removed for a seizure-free outcome) is routinely surgically resected.[3] Although focal seizures are considered to be focal because of their localized onset, they are often associated with a broader epileptogenic network.[4] For example, focal seizures do not always remain in the seizure onset zone (SOZ), often starting in the SOZ and subsequently generalizing to the surrounding cortex (regions outside SOZ [NonSOZ]) in focal epilepsy patients, suggesting the importance of a more distributed epileptic network in seizure propagation.[5–7]

Conventionally, seizure propagation is coordinated by different neuronal oscillations such as low-frequency activity (LFA; <30Hz), high-frequency activity (HFA; >30Hz), or low-to-high cross-frequency coupling (CFC).[6–8] Different neuronal oscillations and their interactions have been suggested to play critical roles in epileptic seizures and could potentially serve as reliable markers for

epileptogenicity and epileptic zones.[9–11] Understanding the network dynamics of seizure evolution is crucial to identifying the functional architecture of each patient's epileptic network, which in turn could lead to improved surgical outcomes.

Two types of seizure propagation dynamics in focal epilepsy patients are of particular interest here: restricted seizure dynamics revealed by focal seizures (Fig 1A) and unrestricted seizure dynamics represented by focal seizures with secondary generalization (see Fig 1B). Previous studies have suggested that seizure propagation is supported by stronger influence from SOZ[12–14] or weaker internal regulation ability from the surrounding regions.[14,15] From the excitation-inhibition interaction perspective, seizure propagation could also be viewed as the result of the SOZ exciting the surrounding cortex or less inhibition coming from the surrounding cortex to the SOZ. Effectively, whether focal seizures secondarily generalize or not depends on the status of bidirectional competition between the SOZ and the surrounding cortex. In line with this notion, we hypothesize that a push–pull antagonism between the

SOZ and the surrounding cortex accounts for differences seen in focal seizure dynamics and that this antagonism is characterized by both within-frequency (LFA or HFA) and cross-frequency (interactions between LFA and HFA) directed information flow (see Fig 1C).

To address and understand these issues, we investigated invasive electrocorticography (ECoG) data from 24 drug-resistant focal epilepsy patients with 54 focal onset seizures and constructed the time-evolving within-frequency and cross-frequency directional interaction networks across preseizure, seizure, and postseizure periods. The within-frequency directional interaction was estimated using the adaptive direct transfer function (ADTF),[5,16] whereas cross-frequency directional interaction was calculated via cross-frequency directionality (CFD).[17] The strength of the push–pull antagonism derived from ADTF and CFD was computed and then compared between the focal epileptic network in focal seizures and the distributed epileptic network in focal seizures that secondarily generalized.

Patients and Methods

Patients

Twenty-four patients (12 male, 12 female, aged 6–46 years; Supplementary Table) with pharmacoresistant epilepsy were included in this study. All patients underwent long-term presurgical monitoring with intracranial electroencephalography at the Mayo Clinic. The ECoG signals were recorded using a Xltek acquisition system (Natus Medical, Oakville, Ontario, Canada) with a 500Hz sampling rate. Subdural grids (4mm diameter contacts with 10mm intercontact spacing), strips, or depth electrodes were implanted on the cortical surface and/or subcortical regions. The scalp suture electrode placed at the vertex was used as the reference for all recordings. Following data acquisition, a notch filter at 60Hz was applied to remove power line noise. Based on visual inspection, channels exhibiting the presence of artifacts were discarded from further analysis. Then, to reduce the contribution to the coupling of the reference channel, we computed the average reference of the data from all remaining channels and subtracted it from each channel to create signals for analysis.[6,13] The study was approved by local institutional review boards at Mayo Clinic and Carnegie Mellon University.

Seizures

Initial clinical markings were made on the ECoG the day of each seizure by a board-certified staff epileptologist responsible for that inpatient's care and were later vetted by another board-certified epileptologist (G.A.W.) with consensus on SOZ, seizure type, and the period between seizure onset, propagation, and termination. We included
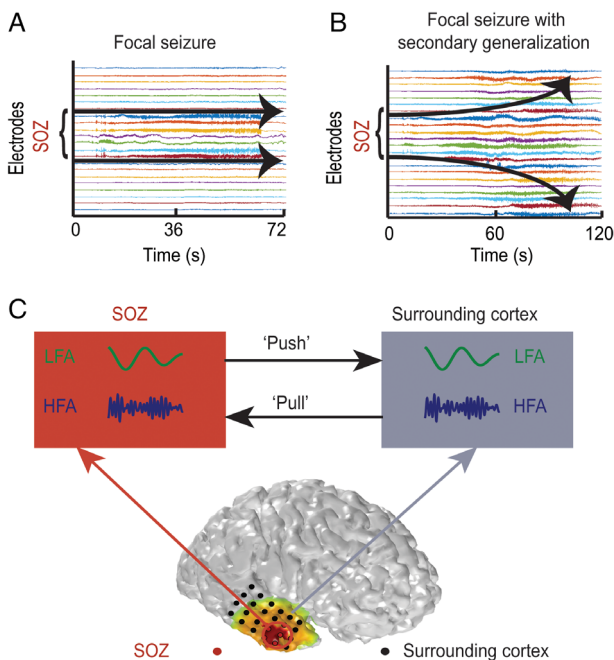

FIGURE 1: Hypothesized seizure regulation mechanism. (A) An example of a focal seizure from Patient 1. The seizure starts at a few channels and remains within a focal area. (B) An example of a focal seizure with secondary generalization from Patient 1. The seizure starts at a few channels and evolves to the broader area. (C) Schematic of the hypothesized seizure regulation mechanism. We hypothesize that the "push–pull" antagonism between the SOZ and the surrounding regions constrains focal seizure secondary generalization, which is further coordinated by both within-frequency (low-frequency activity [LFA] or high-frequency activity [HFA]) and cross-frequency (directional interaction between LFA and HFA) interactions. SOZ = seizure onset zone.
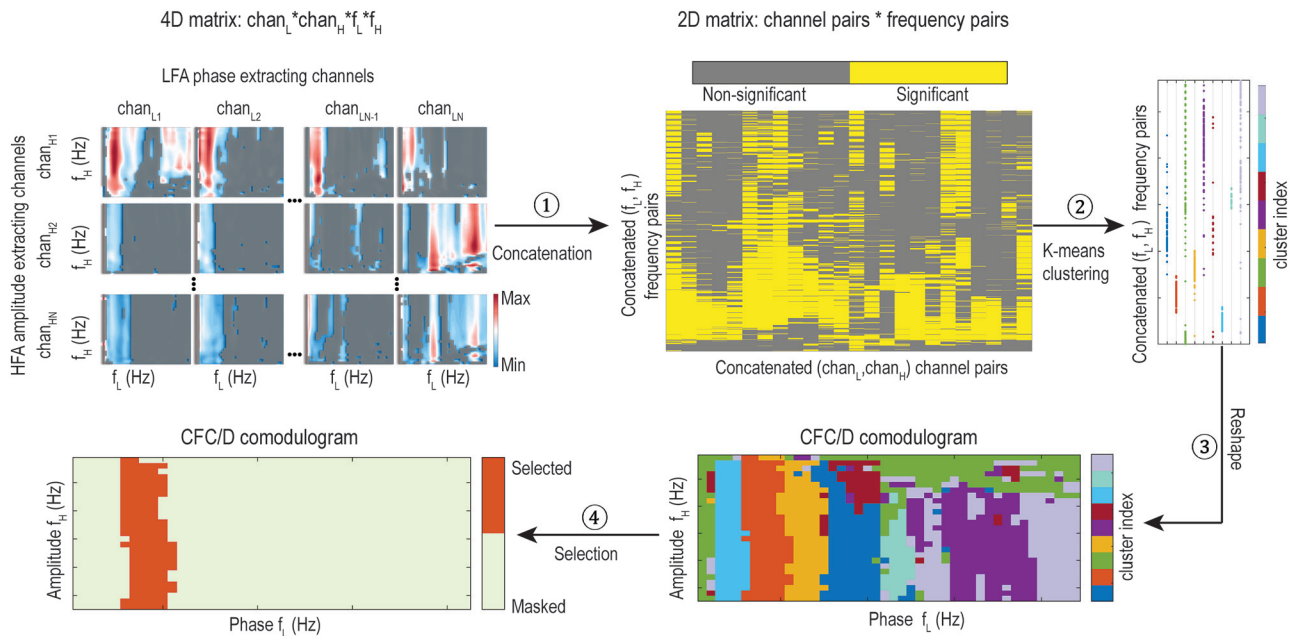
FIGURE 2: Demonstration of cross-channel cross-frequency coupling/directionality (CFC/D) K-means clustering procedure. ① After the surrogate analysis, the nonsignificant elements of 4-dimensional (4D) CFC/D matrix ($chan_L * chan_H * f_L * f_H$) were masked with gray. Then, the binary significance map of 4D CFC/D matrix was transformed to a new 2-dimensional (2D) matrix (*channel pairs * frequency pair*) by concatenating the first 2 dimensions and the last 2 dimensions of the 4D matrix into 1 long vector, respectively. The yellow color codes significant elements, and the gray color codes nonsignificant elements. ② The K-means clustering algorithm partitioned concatenated CFC/D (f_L, f_H) bins by treating channel pairs as variables. After K-means clustering, each element of concatenated (f_L, f_H) frequency pairs was assigned to a cluster and indexed by different colors. ③ The long vector cluster index was reshaped back to the CFC/D comodulograms. ④ The cluster with the largest absolute original CFC/D mean value was selected to represent interactions between low-frequency activity (LFA) or high-frequency activity (HFA). $chan_H$ = the HFA's amplitude extracting channel; $chan_L$ = the LFA's phase extracting channel; f_H = the HFA's amplitude frequency bin; f_L = the LFA's phase frequency bin.

seizures with a focal onset and excluded the seizures that were not localized at onset (eg, poorly localized or seemingly generalized onset seizures by visual inspection of the ECoG). Then, the selected seizures were classified into 2 groups based on clinical seizure semiology. Focal onset seizures were classified as focal aware or focal with impaired awareness based on direct interactions with the patient during the seizures.[18] Focal seizures were identified as the absence of secondarily generalized tonic–clonic clinical correlate; seizures were considered to secondarily generalize if the patient demonstrated tonic–clonic activity. In total, we identified 29 focal seizures (focal onset aware seizures and focal onset with impaired awareness seizures) and 25 focal seizures with secondary generalization (focal to bilateral tonic–clonic seizures). The length of each segment (preseizure, seizure, and postseizure) was determined by the seizure length so that equal distributions of data were used for each class within each patient. The seizure state was defined as onset to ictal, with the pre- (preictal) and postseizure (postictal) states ending and beginning on those time points, respectively. For later connectivity analysis, the ictal period was further evenly divided into early ictal, middle ictal, and late ictal periods with equal intervals.

Within- and Cross-Frequency Connectivity Estimation

The ADTF[19,20] was applied to estimate the within-frequency directed information flow. In contrast to directed transfer function (DTF), ADTF does not assume signal stationarity. Instead, ADTF reconstructed time-variant connectivity patterns by utilizing time-varying coefficients obtained from a multivariate adaptive autoregression and extracted the directed information flow in the frequency domain.[21,22] The within-frequency ADTF information flow was calculated in the following frequency bands: delta (1–4Hz), theta (4–8Hz), alpha (8–13Hz), beta (13–30Hz), low gamma (30–80Hz), and high gamma (80–150Hz) with open-source software eConnetome (https://www.nitrc.org/projects/econnectome/).[23]

Different frequency neuronal oscillations are not independent, and their tendency or extent of interaction is often quantified in terms of CFC. Although CFC has many forms, we are particularly interested in how the phase of LFA modulates the amplitude of HFA due to its robustness of presence across species and conditions.[24,25] The CFC was quantified by calculating the coherence between the phase of LFA and the amplitude of HFA.[26] Moreover, CFD was further applied to evaluate directional
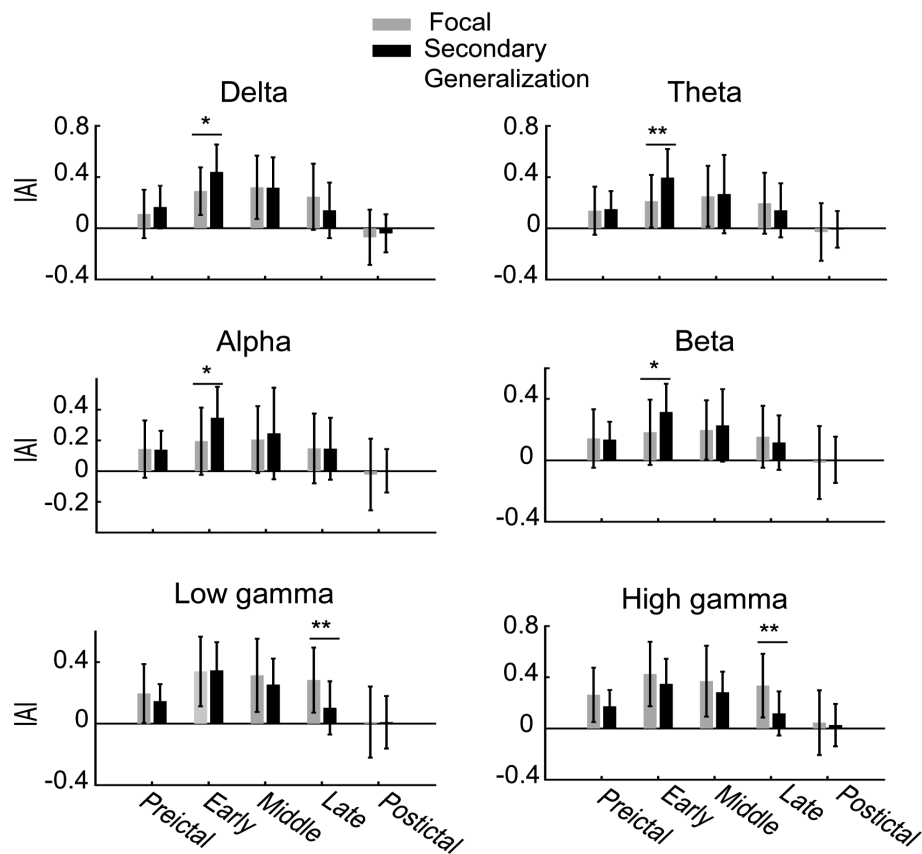
FIGURE 3: Temporal dynamics of within-frequency directed information asymmetry in the delta, theta, alpha, beta, low gamma, and high gamma bands, respectively. Positive information asymmetry index (IAI) value indicates information flow from seizure onset zone (SOZ) to regions outside SOZ (NonSOZ), and negative IAI value indicates information flow from NonSOZ to SOZ. Asterisk indicates *p* < 0.05, and double asterisk indicates *p* < 0.01 (Bonferroni corrected).

interactions between different frequencies by computing the phase–slope index between the phase of LFA and the amplitude envelope of HFA.[17] The phase–slope index is a robust method to quantify directionality because it allows one to infer whether one signal is leading or lagging a second signal by considering the slope of phase differences in a prespecified frequency range.[27] The assumption is that a constant lag in the time domain translates into phase differences, which will change linearly with frequency in the considered range. If the phase slope between LFA's phase and HFA's amplitude envelope is positive, the CFD is positive, suggesting the information flow is from LFA to HFA and vice versa for negative CFD. To reduce interseizure variances, CFC and CFD values are normalized by dividing the maximum absolute value across all periods. Thus, all CFC and CFD values are in the range (0 to 1) and (−1 to 1), respectively.

Surrogate Analysis

To determine if the observed CFC/D modulation was statistically significant, we applied a "circular shift" randomization analysis. During each randomization, we circularly shifted a random number of LFA's phase segments concerning HFA's amplitude envelope segments for each channel, and the CFC/D values for each of the paired channels were recomputed. This procedure was repeated 200 times, resulting in a shuffled CFC/D distribution. Next, the original CFC/D values were compared to their surrogate counterparts, and the *p* value for each element in the CFC/D comodulograms was obtained by extracting its percentile in the shuffled distribution. False discovery rate (FDR) was then performed to correct for multiple comparisons on the resulting *p* values at the *p* = 0.05 level, which controls the rate of significant CFC/D values across all LFA's phase and HFA's amplitude frequency pairs.

K-Means Clustering Analysis

Cross-channel CFC and CFD were computed for all possible channel pairings during the preictal, early ictal, middle ictal, late ictal, and postictal periods, respectively. For each period, a 4-dimensional (4D) CFC/D matrix was formed: $chan_L * chan_H * f_L * f_H$, where $chan_L$ is the LFA's phase extracting channel, $chan_H$ is the HFA's amplitude extracting channel, f_L is the LFA's phase frequency bin,
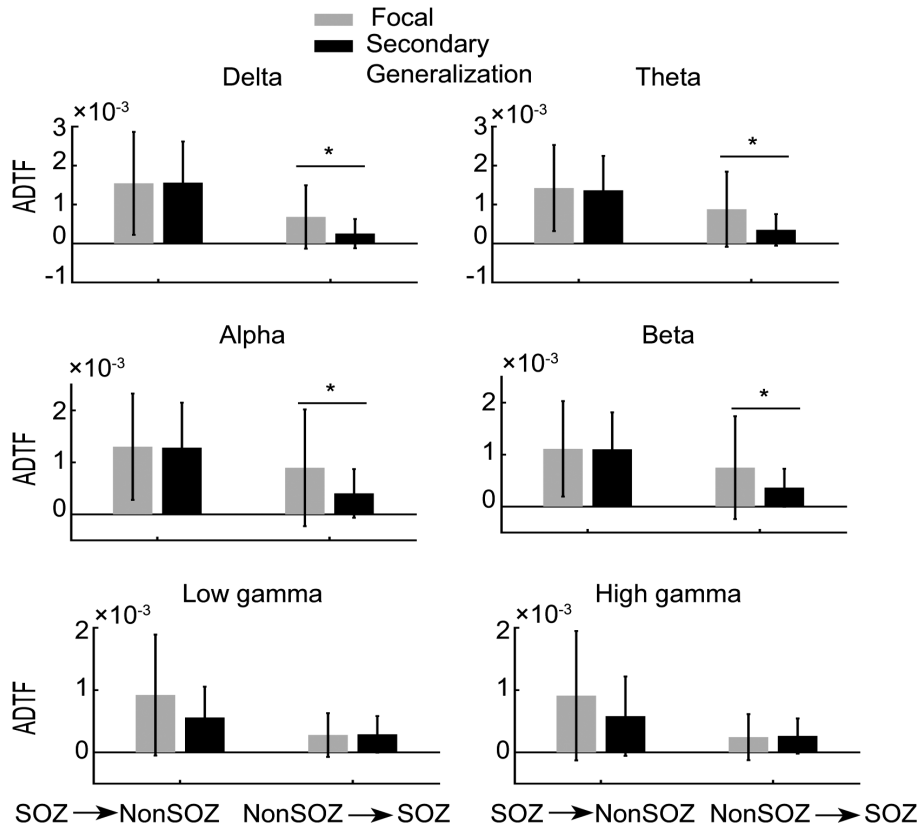
FIGURE 4: The adaptive direct transfer function (ADTF) information flow between seizure onset zone (SOZ) and to regions outside SOZ (NonSOZ) in the delta, theta, alpha, beta, low gamma, and high gamma bands during the identified significantly different information asymmetry index periods, respectively. Asterisk indicates *p* < 0.05.

and f_H is the HFA's amplitude frequency bin. Because CFC/D varied across channel pairs at different levels, we applied a K-means clustering algorithm to identify the most consistent and strongest LFA to HFA CFC/D across all channel pairs (Fig 2). Prior to applying K-means clustering, we conducted a surrogate analysis to assess the significance of CFC/D. Then, the binary significance map of 4D CFC/D matrix was transformed to a new 2-dimensional (2D) matrix by concatenating the first 2 dimensions and the last 2 dimensions of the 4D matrix into 1 long vector, respectively. The rows and columns of the new 2D matrix (*channel pairs * frequency pair*) correspond to the spatial and spectral information. Next, we applied hamming distance in the K-means clustering, and the optimal number of clusters was determined through the Elbow method, which looks at the percentage of variance explained as a function of the number of clusters.[28] If adding another cluster did not give much better modeling of the data and 90% of the variance was explained by the clusters, we chose that number as the appropriate number of clusters. The cluster with the largest absolute CFC/D original mean value was selected to represent interactions between LFA and HFA.

Results

Within-Frequency Directed Information Flow Asymmetry Controls Seizure Dynamics

First, we investigated how within-frequency directional interactions between the SOZ and the NonSOZ constrained seizure propagation. We further defined the information asymmetry index (IAI) as the directional information flow differences between SOZ to NonSOZ and NonSOZ to SOZ, divided by the sum. If IAI was positive, it represented more information flow from SOZ to NonSOZ and vice versa for negative IAI. IAI for all possible SOZ and NonSOZ channel pairs were computed and then averaged. Interestingly, we found IAI was all positive during the preictal and ictal periods for both focal seizures and secondarily generalized seizures in every frequency band (Fig 3). Specifically, IAI was significantly smaller in focal seizures than secondarily generalized seizures in the LFA (delta, theta, alpha, and beta bands) during the early ictal period. On the contrary, IAI was found to be significantly larger in focal seizures comparing to secondarily generalized seizures in the HFA (low gamma and high gamma bands) during the late ictal period. Then, we asked whether the significant IAI differences were due to the influence from SOZ to
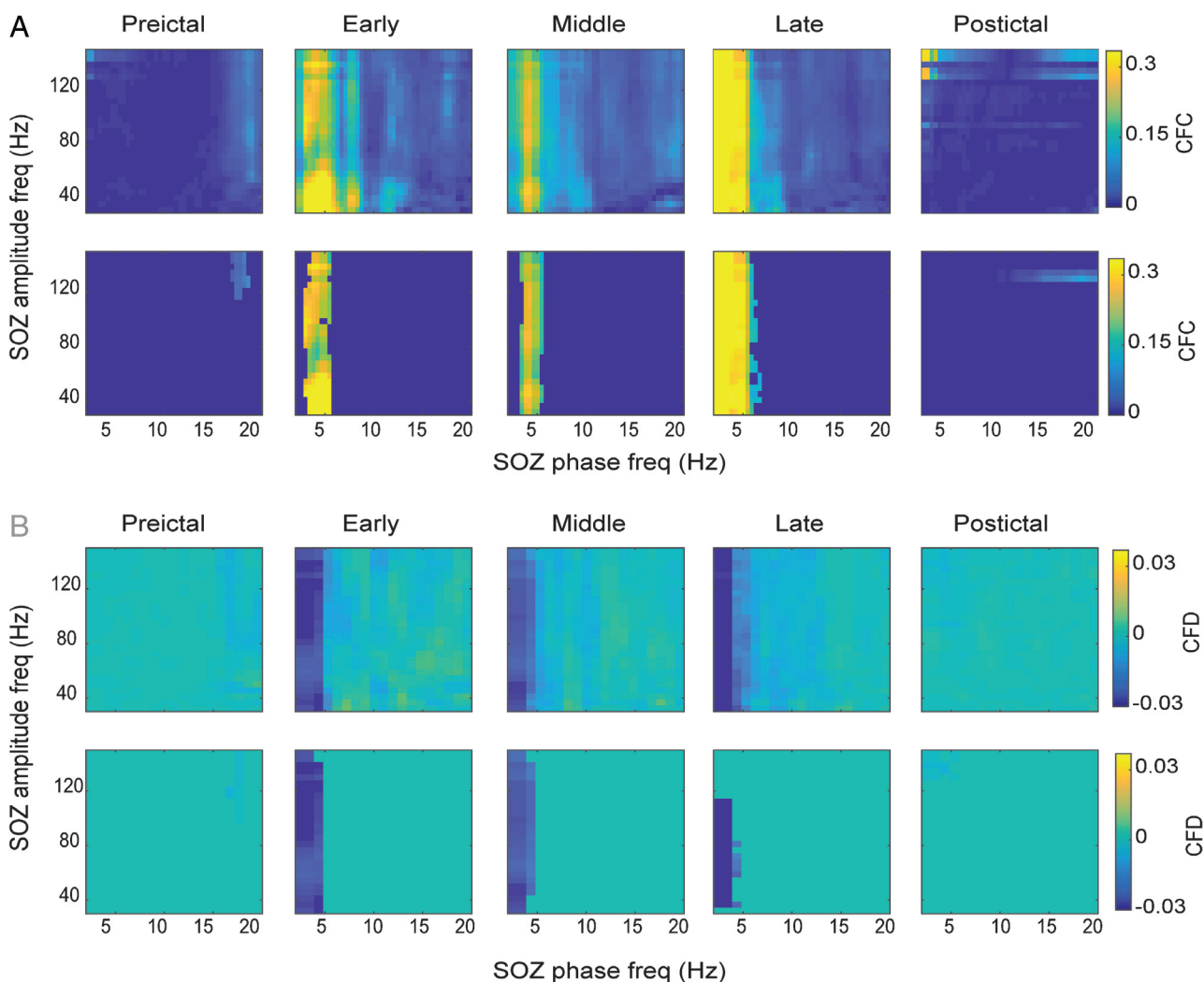
FIGURE 5: Examples of averaged cross-frequency coupling (CFC) and cross-frequency directionality (CFD) comodulograms within seizure onset zone (SOZ) channels and their corresponding K-means clustering results of 1 focal seizure from Patient 3. (A) Top panel: Mean CFC comodulograms within SOZ channels. Bottom panel: CFC comodulograms masked by K means identified the most consistent and strongest CFC cluster. (B) Same as A but for CFD. Positive CFD value indicates information flow from low-frequency activity to high-frequency activity and vice versa for negative CFD value. Freq = frequency.

NonSOZ or the other way around. Notably, directed information from NonSOZ to SOZ in focal seizures was found to be significantly stronger compared to secondarily generalized seizures, and SOZ to NonSOZ directed information flow was not different in the LFA (Fig 4). However, the directed information flow from SOZ to NonSOZ or from NonSOZ to SOZ was not significantly different between focal seizures and secondarily generalized seizures in HFA (low gamma and high gamma bands).

Time-Varying CFC Modulation during Seizure Evolution

To quantify the strength of interaction between LFA and HFA, we computed CFC values between each LFA (2–20Hz, in steps of 1Hz) and HFA (30–150Hz, in steps of 5Hz) in 5 time periods (preictal, early ictal, middle ictal, late

ictal, and postictal periods) across all possible channel pairs for each seizure, constructing the CFC comodulograms. The averaged CFC comodulograms over all SOZ channel pairs and K means derived most consistent and strongest LFA to HFA CFC of a focal seizure from Patient 3 were shown (Fig 5A). The mean CFC values within the representative cluster across all possible channel pairs obtained by K means were used for later statistical analysis. In subregional CFC modulations sorted by SOZ and NonSOZ areas, temporal dynamic characteristic and region specificity was demonstrated (Fig 6). Prominent CFC modulations within SOZ were only present during the seizure period, and the strength was much stronger compared to within NonSOZ (within SOZ = 0.62 ± 0.26; within NonSOZ = 0.25 ± 0.18; $t[106] = 8.58$, $p < 10^{-13}$). When comparing the differences between focal seizures and secondarily generalized seizures, we
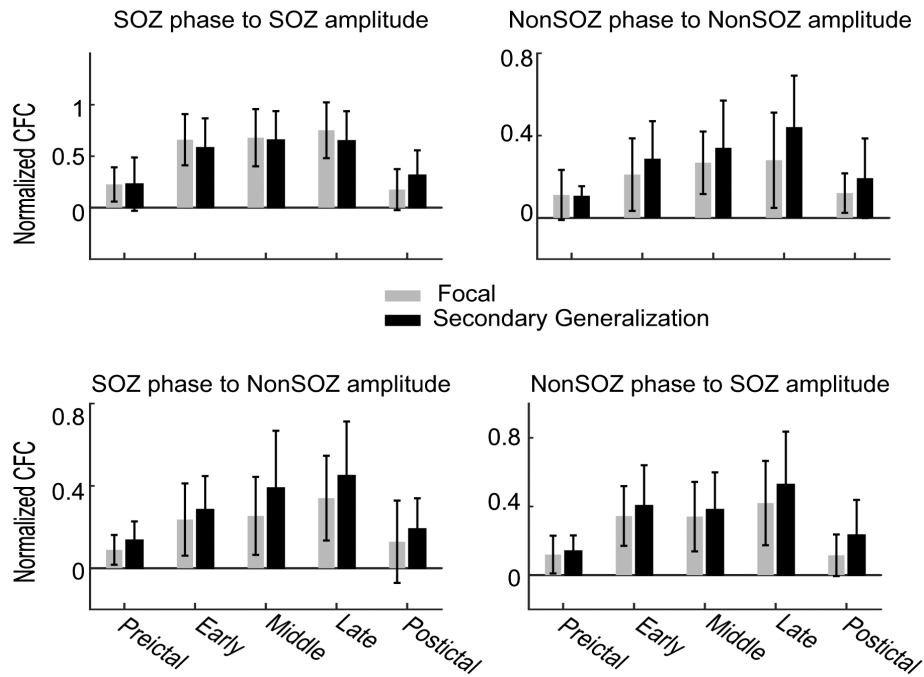
FIGURE 6: Temporal dynamics of cross-frequency coupling (CFC) during the preictal, early ictal, middle ictal, late ictal, and postictal periods. Top left: Low-frequency activity's (LFA) phase from seizure onset zone (SOZ) channels and high-frequency activity's (HFA) amplitude from SOZ channels CFC. Top right: LFA's phase from regions outside SOZ (NonSOZ) channels and HFA's amplitude from NonSOZ channels CFC. Bottom left: LFA's phase from SOZ channels and HFA's amplitude from NonSOZ channels CFC. Bottom right: LFA's phase from NonSOZ channels and HFA's amplitude from SOZ channels CFC. Note that none of these comparisons between 2 seizure types reached significance after multiple comparison correction.
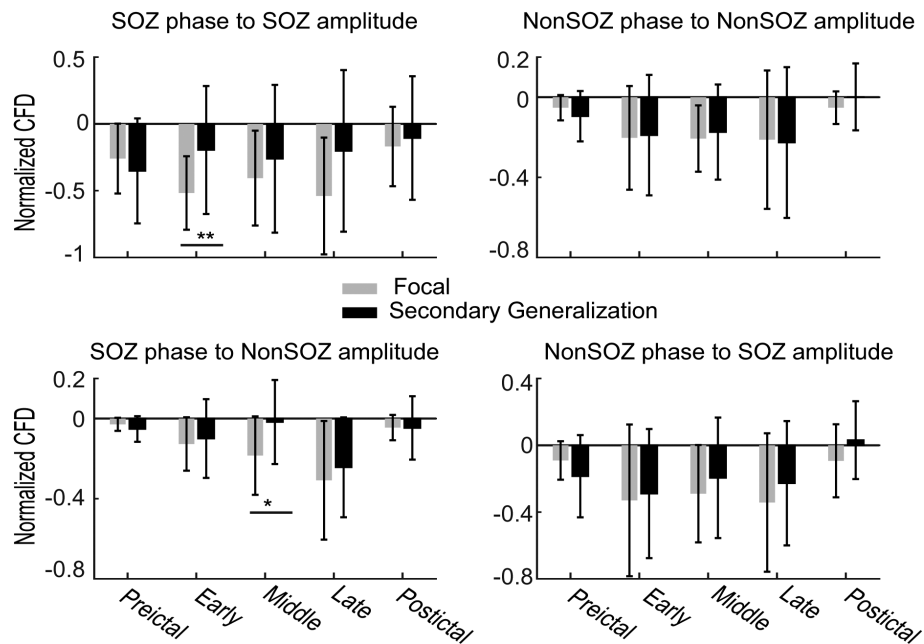

FIGURE 7: Temporal dynamics of cross-frequency directionality (CFD) during the preictal, early ictal, middle ictal, late ictal, and postictal periods. Top left: Low-frequency activity's (LFA) phase from seizure onset zone (SOZ) channels and high-frequency activity's (HFA) amplitude from SOZ channels CFD. Top right: LFA's phase from regions outside SOZ (NonSOZ) channels and HFA's amplitude from NonSOZ channels CFD. Bottom left: LFA's phase from SOZ channels and HFA's amplitude from NonSOZ channels CFD. Bottom right: LFA's phase from NonSOZ channels and HFA's amplitude from SOZ channels CFD. Positive CFD value indicates information flow from LFA to HFA and vice versa for negative CFD. Asterisk indicates $p < 0.05$, and double asterisk indicates $p < 0.01$ (Bonferroni corrected).

did not find any significant CFC differences after correcting for multiple comparisons.

Distinct and Diverse CFD When Focal Seizure Secondarily Generalized

If undirected CFC suggests whether LFA and HFA are communicating or not, CFD could further estimate directionality of this communication between LFA and HFA. The positive CFD value suggested that the information was from the LFA's phase to HFA's amplitude and vice versa for the negative CFD value. The mean CFD comodulograms within SOZ channels and K means derived most consistent and strongest LFA to HFA CFD of a focal seizure from Patient 3 were illustrated (see Fig 5B). After the K-means procedure, we computed the mean CFD in the highlighted LFA and HFA frequency ranges over all possible channel pairs and then conducted statistical analysis. We found 2 significant CFD differences between focal seizures and secondarily generalized seizures after correcting 5 interested time bins with Bonferroni correction (Fig 7). During the early ictal period, both focal seizures and secondarily generalized seizures showed negative CFD values within the SOZ areas (focal seizures = -0.512 ± 0.265; secondarily generalized seizures = -0.202 ± 0.468). In terms of the strength, focal seizures had a significantly more negative CFD compared to secondarily generalized seizures ($t[52] = 3.081$, $p = 0.0165$, Bonferroni corrected). During the middle ictal period, focal seizures showed a more negative CFD value between SOZ's LFA and NonSOZ's HFA versus secondarily generalized seizures ($t[52] = 3.034$, $p = 0.019$, Bonferroni corrected). Because the SOZ's LFA to NonSOZ's HFA CFD in secondarily generalized seizures had effectively a zero mean but large variances (-0.019 ± 0.209), we further investigated CFD signs of each secondarily generalized seizure. When focal seizure was secondarily generalized, 56% of SOZ's LFA to NonSOZ's HFA CFD values were negative, and 44% of them were positive.

Discussion

In the present study, we showed less directed information flow from NonSOZ's LFA to SOZ's LFA during the early ictal period when focal seizures secondarily generalized in the within-frequency scenario. In the cross-frequency situation, secondary generalization was associated with either more information from SOZ's LFA to NonSOZ's HFA or less information flow from NonSOZ's HFA to SOZ's LFA during the middle ictal period. Overall, these results suggest that the competition of information flow between SOZ and NonSOZ constrains secondary generalization dynamics and forms a push–pull antagonism control mechanism coordinated by both within-frequency and cross-frequency

interactions (Supplementary Video), potentially reflecting impaired excitation-inhibition connections in the epileptic network.

Here, we utilized a multilayer network approach, including both within-frequency and cross-frequency network analyses, to investigate the segregation and integration of frequency-specific information in the seizure dynamic. Both when treated as independent frequency bands and when treated as coupled measurements, LFA and HFA have been shown to be effective, robust biomarkers for epilepsy.[8] Given the complexity and variability of the different oscillations involved in seizure dynamics, we computed the ADTF in every frequency band in the within-frequency network. Furthermore, we defined IAI to reflect the directed information flow difference between SOZ and NonSOZ regions and found significantly different IAI in the LFA (delta, theta, alpha, and beta bands) during the early ictal periods between 2 seizure types.

Fundamental work has demonstrated that the distance over which neural populations can synchronize is dependent upon the dominant rhythmic frequency of neural oscillations.[29,30] HFA tends to synchronize neural populations over shorter distances, and LFA tends to synchronize neural populations over longer distances. Moreover, it has also been suggested that inhibitory interneurons provide an important mechanism for synchronization of the neural oscillations of remote neural populations. Thus, the presence of LFA in the long-range communication during the secondary generalization are probably attributable to 2 factors. First, the conduction delay itself lowers the frequency. Second, when there is synchronization across distances, there is an extra inhibitory spike associated with the extra excitation onto the interneurons, and this extra inhibition slows down the next firing of the pyramidal cells.[29] Interestingly, both focal seizures and secondarily generalized seizures showed positive IAI, indicating that the SOZ is always the primary source of information in the widespread epileptic network. This is further supported by numerous studies using directional connectivity to identify SOZ successfully in focal epilepsy patients.[5,31,32] Notably, the IAI differences in the LFA are purely driven by directional interactions from the NonSOZ to SOZ because the magnitude of SOZ to NonSOZ directional connectivity are similar between the 2 types of seizures. As viewed through the push–pull framework, secondary generalization is related to less "pull" from NonSOZ to SOZ, and the "push" from SOZ to NonSOZ remains almost the same in the LFA.

The interactions between LFA and HFA termed as CFC provide a different perspective to investigate the mechanisms of communications across numerous time scales in the epileptic network. It has been suggested that

CFC is a key mechanism in maintaining the inhibition-excitation interaction balance and facilitating cerebral information flow.[33] In epilepsy patients, elevated CFC had been found within SOZ during the ictal period but not the nonictal periods,[34,35] probably indicating a hyperexcitable ictal state.[36] However, CFC is an undirected metric and can only assess the coupling strength, so the directional communication between LFA and HFA is still unknown. Here, we utilized CFD[17] to investigate the directional interactions between LFA and HFA in the epileptic network with a specific focus on focal seizure evolution. At the cellular level, CFD might be associated with the level of pyramidal cell excitatory drive into the pyramidal-interneuron network.[36,37] In the classical CFC theory, it has been proposed that pulse of inhibition paced at LFA and targeted at the generators of HFA[38–40]: when LFA paced inhibition starts to ramp down, the fast-spiking interneurons would start firing. In this case, the information flow is from LFA to HFA (positive CFD). Conversely, if the excitatory drive of the pyramidal cells is strong enough, this high excitation would overcome the inhibition paced at LFA earlier and alter the relative firing timing of LFA and HFA. In this situation, the information flow is from HFA to LFA (negative CFD). Taken together, the directional information flow between LFA and HFA reflected by CFD might implicate an effective excitation/inhibition ratio in the pyramidal-interneuron interaction network.

The applications of CFD have proven to be powerful across different electrophysiological modalities including ECoG,[41] electroencephalogram,[42,43] and magnetoencephalography,[44] often revealing bold new insights. In our CFD analysis, we found significant CFD differences within the SOZ during early ictal periods between the 2 types of seizures, with CFD being more negative in focal seizures compared to secondarily generalized seizures (see Fig 7, top left panel). In cross-regional interactions between SOZ and NonSOZ, CFD values between the SOZ's LFA and NonSOZ's HFA were significantly different during the middle ictal period (see Fig 7, bottom left panel). High negative CFD values between SOZ's LFA and NonSOZ's HFA in focal seizures indicated cross-frequency directional information flow from NonSOZ's HFA to SOZ's LFA, reflecting strong "pull" from NonSOZ to SOZ, which eventually prevented secondary generalization. Interestingly, CFD between SOZ's LFA and NonSOZ's HFA in secondarily generalized seizures is more complex and diverse, which could be either negative or positive (Fig 8). When CFD values between SOZ's LFA and NonSOZ's HFA in secondarily generalized seizures were negative but attenuated (see Fig 8B), there was insufficient "pull" from the NonSOZ to SOZ to stop seizure propagation. In contrast, when SOZ's LFA to NonSOZ's HFA CFD was
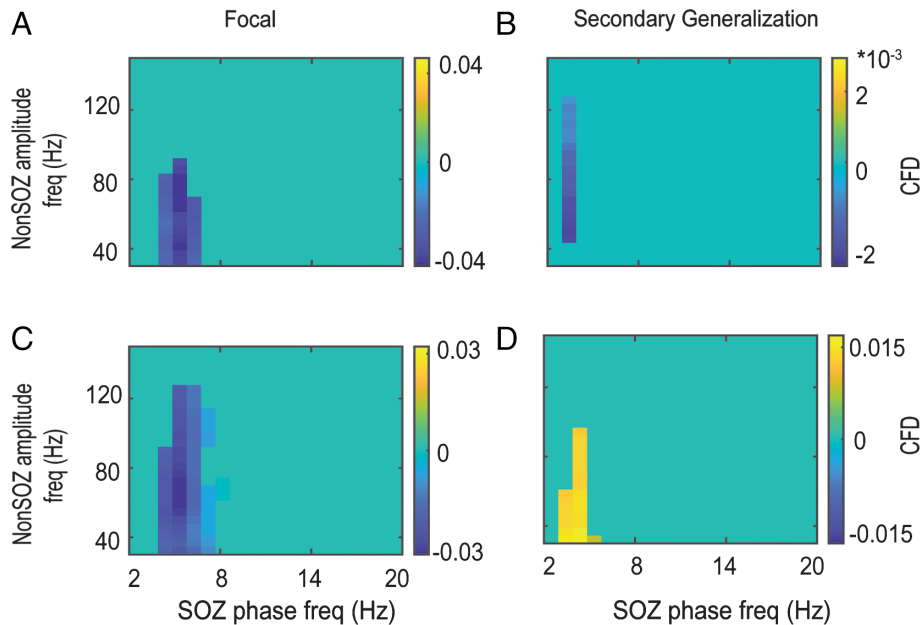

FIGURE 8: Example of 2 distinct cross-frequency directionality (CFD) patterns between seizure onset zone's (SOZ) low-frequency activity (LFA) and regions outside SOZ's (NonSOZ) high-frequency activity (HFA) during the middle ictal period when focal seizures were secondarily generalized. CFD comodulograms were masked after the K-means clustering. An example of (A) a focal seizure and (B) a secondarily generalized seizure from Patient 1. The less negative CFD indicated reduced information flow from NonSOZ's HFA to SOZ's LFA when focal seizure was secondarily generalized. An example of (C) a focal seizure and (D) a secondarily generalized seizure from Patient 24. The positive CFD indicated information flow from SOZ's LFA to NonSOZ's HFA when focal seizure secondarily generalized. freq = frequency.

positive in secondarily generalized seizures (see Fig 8D), the cross-frequency information flow was from SOZ's LFA to NonSOZ's HFA, suggesting SOZ "push" to NonSOZ. In connection with the neurophysiological underpinnings of CFD, the secondary generalization of focal seizure might be modulated by the level of an excitatory pyramidal drive into the pyramidal-interneuron network outside SOZ and is manifested by LFA to HFA CFD dynamics.

There were a few prior studies investigating the dynamics of seizure generation and evolution. Chang et al found that the transition from interictal to seizure is modulated by interictal epileptiform discharges, which produce phasic changes in the slow transition process and exert opposing effects on the dynamics of a seizure-generating network, causing either antiseizure or proseizure effects.[45] Here, we focused on the mechanism of seizure evolution dynamics after generation rather than seizure emergence. Khambhati et al proposed a push–pull antagonism in regulating seizure evolution by constructing the functional connectivity network in the high gamma band.[6] Although inspired by this seminal work on a push–pull control mechanism, our study is advanced in 2 main aspects. First, we established a directional connectivity network instead of a functional connectivity network. Unlike functional connectivity, directional connectivity allows for identification of the driving source. Second, we utilized a multilayer network approach to uncover a complete picture of epilepsy network in secondary generalization dynamics, which requires integration of oscillations across the full frequency spectrum, as well as cross-frequency interaction. In an animal study, Liou et al combined multimodal imaging and pharmacological manipulation to investigate focal seizure propagation pathways.[46] They induced focal seizures in the rodent with the 4-aminopyridine (4-AP) model and used bicuculline methiodide, a γ-aminobutyric acid (GABA)-A receptor antagonist, to block GABA-A activity and impair local inhibition outside of the 4-AP focus at varying distances. It was hypothesized that although the strongly excitatory synaptic projections that had originated from the seizure focus were widely distributed, they were masked by surrounding inhibitory responses. When the inhibition in the surrounding cortex was compromised, the seizure propagated. Therefore, they concluded that surrounding inhibitory activity impedes the secondary generalization and spread of focal seizures. In our human epileptic seizure study, focal seizure evolution was mainly determined by regions outside SOZ in the within-frequency and cross-frequency information flow dynamics carried by LFA and HFA. Therefore, comprised surrounding inhibitory control might provide an alternative and plausible mechanism to explain focal seizure dynamics at the neuronal population level in the human focal epilepsy. Moreover, Schevon et al reported an inhibitory restraint mechanism of seizure activity from multielectrode array (MEA) recordings in the presumptive neocortical SOZ.[47] As compared with MEA recordings, which offer merits in revealing the very HFA, ECoG recordings mainly reflect the postsynaptic potential activity in the low-frequency range and may not provide the actual location of seizure activity as accurately as MEA. Schevon et al demonstrated that there is a sharp delineation between areas showing intense, hypersynchronous firing indicative of recruitment to the seizure and adjacent "ictal penumbra" territories where there are large-amplitude ECoG signals, reflecting feedforward synaptic currents, but with low-level local firing. Therefore, it is possible that the synaptic spread from the ictal focus could be extended to the distant broader areas outside SOZ, which provides an alternative explanation for our findings.

The major limitation in the present study is the sparse spatial sampling and the error inherent in any epilepsy intracranial implantation procedure. Our findings are limited to the cortical areas covered by the ECoG grids or penetrating depth electrodes that target mesial temporal structures (hippocampus and amygdala), although previous studies have suggested that subcortical regions are crucial for seizure maintenance[48,49] and impairment of awareness.[50] For this reason, care must be given in the interpretation of results because subcortical seizure propagation is potentially a critical distinguishing factor as well. Future studies may investigate the cortical and subcortical network interactions using stereotactic electroencephalography that include thalamic targets.

In conclusion, the secondary generalization of human epileptic focal seizure is constrained by multiple oscillatory push–pull antagonistic interactions between the SOZ and the surrounding regions and is coordinated by both within-frequency and cross-frequency directional interactions. These results further suggest that a promising biomarker for the secondary generalization of focal seizures is an imbalance in excitation-inhibition activity within the epileptic network. Additionally, this push–pull control mechanism appears to be primarily modulated by regions outside of the SOZ. Further research is needed to evaluate whether increasing regulation over regions outside of the SOZ is an effective treatment for epileptic patients.

Acknowledgment

Author Contributions

H.J. and B.H. contributed to the conception and design of the study. H.J., Z.C., G.A.W., and B.H. contributed to the acquisition and analysis of data. H.J. and B.H. contributed the drafting of the manuscript text. All authors approved the final version of the manuscript.

Potential Conflicts of Interest

Nothing to report.

References

1. Sander JW, Shorvon SD. Epidemiology of the epilepsies. J Neurol Neurosurg Psychiatry 1996;61:433–443.

2. Kutsy RL, Farrell DF, Ojemann GA. Ictal patterns of neocortical seizures monitored with intracranial electrodes: correlation with surgical outcome. Epilepsia 1999;40:257–266.

3. Kuzniecky R, Devinsky O. Surgery insight: surgical management of epilepsy. Nat Clin Pract Neurol 2007;3:673–681.

4. Naftulin JS, Ahmed OJ, Piantoni G, et al. Ictal and preictal power changes outside of the seizure focus correlate with seizure generalization. Epilepsia 2018;59:1398–1409.

5. Wilke C, Worrell G, He B. Graph analysis of epileptogenic networks in human partial epilepsy. Epilepsia 2011;52:84–93.

6. Khambhati AN, Davis KA, Lucas TH, et al. Virtual cortical resection reveals push-pull network control preceding seizure evolution. Neuron 2016;91:1170–1182.

7. Burns SP, Santaniello S, Yaffe RB, et al. Network dynamics of the brain and influence of the epileptic seizure onset zone. Proc Natl Acad Sci U S A 2014;111:E5321–5330.

8. Guirgis M, Chinvarun Y, Del Campo M, et al. Defining regions of interest using cross-frequency coupling in extratemporal lobe epilepsy patients. J Neural Eng 2015;12:026011.

9. Tao JX, Chen XJ, Baldwin M, et al. Interictal regional delta slowing is an EEG marker of epileptic network in temporal lobe epilepsy. Epilepsia 2011;52:467–476.

10. Brigo F. Intermittent rhythmic delta activity patterns. Epilepsy Behav 2011;20:254–256.

11. Jacobs J, Staba R, Asano E, et al. High-frequency oscillations (HFOs) in clinical epilepsy. Prog Neurobiol 2012;98:302–315.

12. Kramer MA, Cash SS. Epilepsy as a disorder of cortical network organization. Neuroscientist 2012;18:360–372.

13. Kramer MA, Eden UT, Kolaczyk ED, et al. Coalescence and fragmentation of cortical networks during focal seizures. J Neurosci 2010;30:10076–10085.

14. Schindler KA, Bialonski S, Horstmann MT, et al. Evolving functional network properties and synchronizability during human epileptic seizures. Chaos 2008;18:033119.

15. Bower MR, Stead M, Meyer FB, et al. Spatiotemporal neuronal correlates of seizure generation in focal epilepsy. Epilepsia 2012;53:807–816.

16. Wilke C, Ding L, He B. Estimation of time-varying connectivity patterns through the use of an adaptive directed transfer function. IEEE Trans Biomed Eng 2008;55:2557–2564.

17. Jiang H, Bahramisharif A, van Gerven MA, Jensen O. Measuring directionality between neuronal oscillations of different frequencies. NeuroImage 2015;118:359–367.

18. Fisher RS, Cross JH, French JA, et al. Operational classification of seizure types by the International League Against Epilepsy: position paper of the ILAE Commission for Classification and Terminology. Epilepsia 2017;58:522–530.

19. Ding M, Bressler SL, Yang W, Liang H. Short-window spectral analysis of cortical event-related potentials by adaptive multivariate autoregressive modeling: data preprocessing, model validation, and variability assessment. Biol Cybern 2000;83:35–45.

20. Wilke C, Ding L, He B. An adaptive directed transfer function approach for detecting dynamic causal interactions. Conf Proc IEEE Eng Med Biol Soc 2007;2007:4949–4952.

21. Ding L, Worrell GA, Lagerlund TD, He B. Ictal source analysis: localization and imaging of causal interactions in humans. NeuroImage 2007;34:575–586.

22. Ding M, He B. Exploring functional and causal connectivity in the brain. In: He B, ed. Neural engineering. Boston, MA: Springer US, 2013.

23. He B, Dai Y, Astolfi L, et al. eConnectome: A MATLAB toolbox for mapping and imaging of brain functional connectivity. J Neurosci Methods 2011;195:261–269.

24. Canolty RT, Knight RT. The functional role of cross-frequency coupling. Trends Cogn Sci 2010;14:506–515.

25. Jensen O, Colgin LL. Cross-frequency coupling between neuronal oscillations. Trends Cogn Sci 2007;11:267–269.

26. Osipova D, Hermes D, Jensen O. Gamma power is phase-locked to posterior alpha activity. PLoS One 2008;3:e3990.

27. Nolte G, Ziehe A, Nikulin VV, et al. Robustly estimating the flow direction of information in complex physical systems. Phys Rev Lett 2008;100:234101.

28. Thorndike RL. Who belongs in the family. Psychometrika 1953;18:267–276.

29. Kopell N, Ermentrout GB, Whittington MA, Traub RD. Gamma rhythms and beta rhythms have different synchronization properties. Proc Natl Acad Sci U S A 2000;97:1867–1872.

30. Brunel N, Wang XJ. What determines the frequency of fast network oscillations with irregular neural discharges? I. Synaptic dynamics and excitation-inhibition balance. J Neurophysiol 2003;90:415–430.

31. van Mierlo P, Carrette E, Hallez H, et al. Ictal-onset localization through connectivity analysis of intracranial EEG signals in patients with refractory epilepsy. Epilepsia 2013;54:1409–1418.

32. Wilke C, van Drongelen W, Kohrman M, He B. Neocortical seizure foci localization by means of a directed transfer function method. Epilepsia 2010;51:564–572.

33. Onslow AC, Jones MW, Bogacz R. A canonical circuit for generating phase-amplitude coupling. PLoS One 2014;9:e102591.

34. Ibrahim GM, Wong SM, Anderson RA, et al. Dynamic modulation of epileptic high frequency oscillations by the phase of slower cortical rhythms. Exp Neurol 2014;251:30–38.

35. Zhang R, Ren Y, Liu C, et al. Temporal-spatial characteristics of phase-amplitude coupling in electrocorticogram for human temporal lobe epilepsy. Clin Neurophysiol 2017;128:1707–1718.

36. Grigorovsky V, Bardakjian BL. Low-to-high cross-frequency coupling in the electrical rhythms as biomarker for hyperexcitable neuroglial networks of the brain. IEEE Trans Biomed Eng 2018;65:1504–1515.

37. Tort AB, Rotstein HG, Dugladze T, et al. On the formation of gamma-coherent cell assemblies by oriens lacunosum-moleculare interneurons in the hippocampus. Proc Natl Acad Sci U S A 2007;104:13490–13495.

38. Kopell N, Börgers C, Pervouchine D, et al. Gamma and theta rhythms in biophysical models of hippocampal circuits. In: Cutsuridis V, Graham B, Cobb S, Vida I, eds. *Hippocampal microcircuits: a computational modeler's resource book.* New York, NY: Springer New York, 2010.

39. Tort AB, Scheffer-Teixeira R, Souza BC, et al. Theta-associated high-frequency oscillations (110-160Hz) in the hippocampus and neocortex. Prog Neurobiol 2013;100:1–14.

40. Stacey WC, Lazarewicz MT, Litt B. Synaptic noise and physiological coupling generate high-frequency oscillations in a hippocampal computational model. J Neurophysiol 2009;102:2342–2357.

41. Zheng J, Anderson KL, Leal SL, et al. Amygdala-hippocampal dynamics during salient information processing. Nat Commun 2017;8:14413.

42. Helfrich RF, Mander BA, Jagust WJ, et al. Old brains come uncoupled in sleep: slow wave-spindle synchrony, brain atrophy, and forgetting. Neuron 2018;97:221–230.

43. Helfrich RF, Huang M, Wilson G, Knight RT. Prefrontal cortex modulates posterior alpha oscillations during top-down guided visual perception. Proc Natl Acad Sci U S A 2017;114:9457–9462.

44. Park H, Lee DS, Kang E, et al. Formation of visual memories controlled by gamma power phase-locked to alpha oscillations. Sci Rep 2016;6:28092.

45. Chang WC, Kudlacek J, Hlinka J, et al. Loss of neuronal network resilience precedes seizures and determines the ictogenic nature of interictal synaptic perturbations. Nat Neurosci 2018;21:1742–1752.

46. Liou JY, Ma H, Wenzel M, et al. Role of inhibitory control in modulating focal seizure spread. Brain 2018;141:2083–2097.

47. Schevon CA, Weiss SA, McKhann G Jr, et al. Evidence of an inhibitory restraint of seizure activity in humans. Nat Commun 2012;3:1060.

48. Paz JT, Davidson TJ, Frechette ES, et al. Closed-loop optogenetic control of thalamus as a tool for interrupting seizures after cortical injury. Nat Neurosci 2013;16:64–70.

49. Aupy J, Wendling F, Taylor K, et al. Cortico-striatal synchronization in human focal seizures. Brain 2019;142:1282–1295.

50. Motelow JE, Li W, Zhan Q, et al. Decreased subcortical cholinergic arousal in focal seizures. Neuron 2015;85:561–572.